

Article citation info:

Hu Y, Yang H, Ge H, Hua Y, Jin H, Pan K, Life prediction and risk assessment on the aircraft cable based on thermal damage features, *Eksploracja i Niezawodność – Maintenance and Reliability* 2024; 26(4) <http://doi.org/10.17531/ein/191696>

Life prediction and risk assessment on the aircraft cable based on thermal damage features

Indexed by:



Yinxiao Hu^a, Haoqi Yang^a, Hongjuan Ge^{a,*}, Yingchun Hua^b, Hui Jin^a, Kuangming Pan^a

^a Nanjing University of Aeronautics and Astronautics, China

^b Civil Aviation Management Institute of China, China

Highlights

- Two types of thermal damage features are defined based on the mechanism of cable thermal damage.
- Combined with FIDES and thermal damage influence factor, a more accurate cable life prediction method is proposed.
- The cable dynamic risk model is constructed with radial melting rate.

Abstract

Aiming at the operational risk caused by melting of aircraft cable insulation layer, an aircraft cable safety analysis method based on thermal damage characteristics is proposed. Based on the mechanism of cable thermal damage, two types of damage characteristics are defined, which characterize the influence and degree of cable thermal damage. Use thermal damage influence factor to indicate that cable thermal damage accelerates cable failure, and a method of cable life prediction is proposed. Meanwhile, the proportion coefficient μ is set to evaluate the applicability of the life prediction method. The life prediction results show that the cable life prediction method proposed owes higher accuracy, and comparison results show that the proposed method $MTBF_1$ is more applicable in different operating areas. Moreover, a dynamic risk assessment model for aircraft cable is constructed from two perspectives, and the failure probability of cable is modified by the thermal damage influence factor. The risk assessment result is consistent with the experimental, which proves the effectiveness of the model.

Keywords

aircraft cable, life prediction, risk assessment, thermal damage factor, radial melting rate

This is an open access article under the CC BY license (<https://creativecommons.org/licenses/by/4.0/>)

1. Introduction

The temperature change of the aircraft cable insulation layer directly affects the performance of the cable. When the temperature reaches the melting point, the insulation layer melts, the insulation performance of the cable decreases, the current carrying capacity is weakened, and even abnormal conditions such as leakage and short circuits are generated, which endangers the operation of the aircraft [1-2]. With the development of civil aircraft multi-electric technology, the type and power of airborne equipment are increased, and the energy transmission density of cables is continuously improved, which

puts forward higher requirements for the security level and risk identification of cable [3-4].

Domestic and foreign scholars have carried out extensive research on cable safety, especially the influence of thermal environment on cable safety. Zhang Yuemei [5-6] establishes the cable failure physical equation based on the coupling relationship between heat, electricity and vibration, and constructs the cable life prediction model by introducing different factor weights in combination with the support vector machine. Meanwhile, when estimating cable failure parameters

(*) Corresponding author.

E-mail addresses:

Y. Hu (ORCID: 0009-0004-1629-6544) yxhu601@nuaa.edu.cn, H. Yang yhq970429@nuaa.edu.cn,
H. Ge (ORCID: 0000-0003-0376-9803) gehongjuan1101a@nuaa.edu.cn, Y. Hua huayingchun@yahoo.com.cn,
H. Jin jin_hui@nuaa.edu.cn, K. Pan pankuangming@nuaa.edu.cn,

by Bayesian, she introduces uncertainty factors to establish a nonlinear hybrid model containing prior information, which significantly improves the accuracy of failure efficiency parameter estimation. Gen Zhao and Haibo Di [7] divide the working state of the cable into five levels based on the cable state parameters including current, voltage, voltage deviation and three-phase unbalance and the weights obtained from the comparison of the parameters, and further proposed the cable health assessment method based on the matter-element extension model. Salem Okpokparoro and Srinivas Sriramula[8] analyze the mechanical characteristics of submarine cables. Based on the construction and dynamic simulation of cable power load model, the short-term and long-term fatigue damage characteristics and reliability variation relationship of cables are analyzed with wind and wave as the main influencing factors combined with the Kriging model. Mahipal Bukya and Rajesh Kumar[9] take the safety of high-voltage Direct current cables for electric vehicles as the research object, analyze the radial distribution of electrical stress, and the relationship between conductivity and insulation performance with temperature. B. Diban and G. Mazzanti[10] analyze the influence of temperature and electric field distribution on cable insulation performance, and research the cable reliability estimation and life prediction methods affected by electrical stress and temperature stress. Yang Ping [11] considers the influence of the space charge accumulation effect on cable insulation failure, carries out a cable electroacoustic pulse test, determines the average space charge density as a significant cable performance attenuation parameter, and further proposes a cable performance attenuation model. Yanqun Liao and Shuzhen Bao[12] take the 220kV cable joint fault as the research object, construct a simulation model of mechanical stress, pulse voltage and electric tree growth, and carry out material performance test to verify the validity of the simulation model. He Zhu and Zhaobing Han[13] construct the finite element model of the parallel buried cable to analyze the influence of soil properties, ambient temperature, cable distance and other factors on the thermal stress and temperature of the cable, and design orthogonal experiments to compare the influence degree of different cable influence factors. Ma Long and Hu Fang[14] take fiber optic cable as the research object, and the failure statistics show that thermal stress is the main cause of cable

failure. The fiber optic cable performance degradation model obtained by accelerated test and the particle filter algorithm is used to predict the actual operating life of the fiber optic cable. The above researches make contributions to cable safety analysis by establishing the safety evaluation model according to the variation of cable performance parameters. However, there are almost no researches about the definition of cable thermal damage features, and the research reports on introducing changes in thermal damage characteristics into life prediction and risk assessment.

In recent years, the rapid development of artificial intelligence has provided new ideas for the life prediction of electronic equipment, including cables [15-16]. For cable life prediction, T.V.Santhosh and V.Gopika [17] introduce convolutional neural networks into the reliability prediction of nuclear engineering cables, and analyze the relationship between cable life and temperature by small sample cable accelerated life testing data. Qiaosheng Pan and Chi Zhang [18] propose a method for evaluating and classifying cable safety state based on the PSO-XGBoost model and monitoring data such as lifetime and partial discharge amount, using underground cables as the research object. Yang Hu and Chizhi Huang [19] introduce the BP neural network model into cable life estimation, and combine the parameters of cable mechanical properties, material properties and electrical characteristics to achieve cable life prediction with smaller errors. Li Dengshu and Wang Xin [20], based on the data of multiple cable insulation test items, introduce the least square support vector regression algorithm into the main feature analysis of cable life, and further carry out the study of cable life prediction through the partial least square algorithm. Meanwhile, the feature-based life prediction method with the battery as the typical research object has been widely and deeply studied. Gao Jingyi and Yang Dongfang [21] propose a battery health state estimation framework combining Mixers and bidirectional time convolutional neural networks, which provide a basis for battery life prediction. Liu Yanshuo and Li Qiang [22] take electrochemical impedance spectroscopy as the starting point and propose a method of characteristic extraction of electrochemical impedance spectroscopy and prediction of battery life characteristics by combining variational autoencoder and bidirectional gated cycle unit, which further

improves the efficiency of life prediction. Pengya Fang and Xiaoxiao Sui [23] establish the spatio-temporal relationship of cable life by using one-dimensional convolutional neural networks on the basis of battery life feature extraction, and analyze the remaining life of lithium-ion batteries by the short-duration neural network. Some scholars have also introduced support vector regression [24], echo state network [25] and other algorithms into the research of battery life prediction, providing a reference for the life prediction of electronic devices such as cables. The above intelligent algorithm provides a new idea for cable safety state evaluation and cable life prediction. Regrettably, it requires high data quality and quantity, and may be challenging in practice.

Based on the existing researches, we propose a cable life prediction and risk assessment method combined with cable thermal damage characteristics, which requires less cable characteristic data, and the results of life prediction and risk

assessment are more accurate. The method proposed in this paper is shown in Fig.1. Based on the thermal damage mechanism of the cable insulation layer, two types of cable damage characteristics are defined including the influence factor of cable thermal damage and the radial melting rate, which is described in detail in the Sec.2. Then the cable failure probability model combined with the performance attenuation factor, and further the life prediction is carried out in Sec.3. Moreover, the dynamic assessment of cable risk combined with cable failure probability and melting rate of thermal damage is carried out in Sec.4. Finally we summarize the contents and gives a prospect in Sec.5 . The proposed cable life prediction method and a dynamic risk assessment model may support the safety analysis and airworthiness certification of aircraft cables, and could provide a reference for the safety evaluation of other systems.

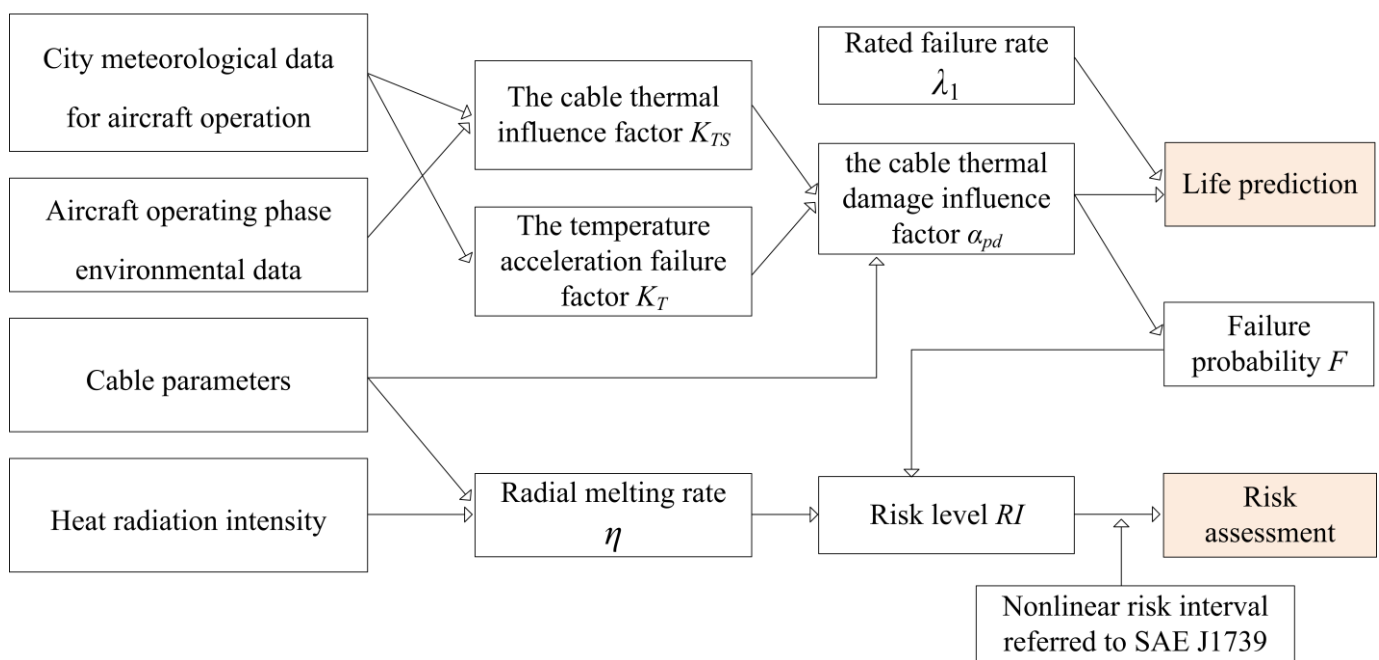


Fig.1. The process of proposed life prediction and risk assessment.

2. Definition of cable damage characteristics based on thermal damage mechanism

2.1. Model Assumptions

Literature [26] lists the operation life of a certain type of aircraft cable in different regions, the cable failure rate follows an exponential distribution, and the rated failure rate has been given. We take it as the research object and use the following assumptions to improve the efficiency of the analysis:

i) Each core of multi-core cables is identical so that the multi-core cables can be simplified into single-core cables with equal cross-sectional areas [27], and the cable is divided into two parts: insulation layer and conductor, where insulation consists of the outer sheath, internal insulation materials, and so on [28].

ii) Since the melting point of the conductor is much higher than the melting point of the insulation layer, only consider the melting of the insulation layer, and ignore the melting of the conductor.

iii) The cables analyzed are arranged along the fuselage, and assume that the initial temperature on the outer surface of the insulation layer of the aircraft cable is approximately equal to the ambient temperature.

iv) The durability test, fatigue test and other environmental tests have been carried out, so that the rated failure rate has considered the influence of conductor heating on the insulation layer [29]. Therefore, the conductor's thermal power is ignored.

2.2. Cable thermal damage mechanism

Affected by internal and external environment and other factors, on the one hand, the cable temperature rise causes the polymer

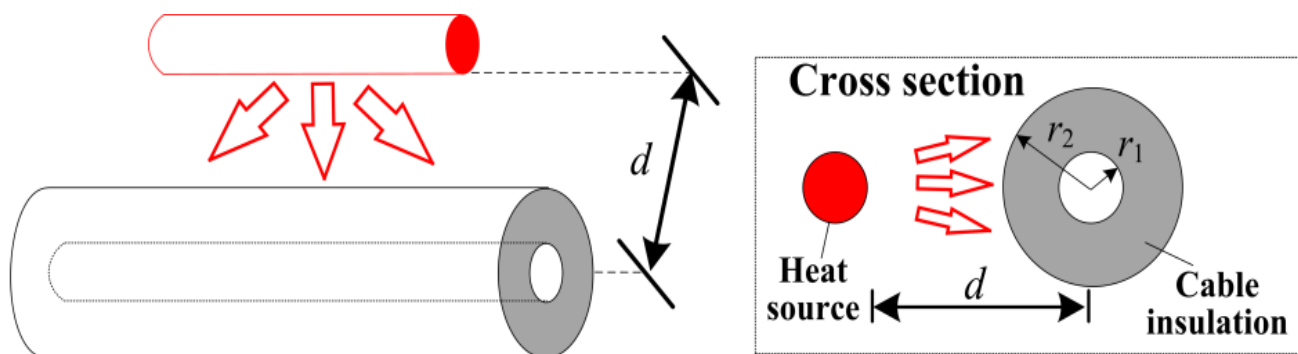


Fig.2. Simplified model of cable heat absorption.

The change rate of heat absorption depends on the ambient thermal power P_{heat} and the already absorbed heat E_s for aircraft cable, which approximately satisfies the energy balance relationship [30] :

$$\frac{dE_s}{dt} = \gamma P_{heat} - \alpha E_s \quad (1)$$

Where γ is the environmental heat transfer coefficient and α is the heat absorption coefficient of the aircraft cable. When the change rate of E_s is 0, the heat absorbed by the aircraft cable has reached saturation, and the heat absorption equation of the cable is solved as follows.

$$E_s = \left(\frac{\gamma P_{heat}}{\alpha}\right)[1 - e^{(-\alpha t)}] \quad (2)$$

Due to the small heat capacity, small insulation layer and limited heat absorption of aircraft cable, it is approximately considered that the cable temperature change time is very short. A simplified cable heat absorption equation is obtained by eliminating the higher order infinite minor term of equation (2) by Taylor expansion:

$$E_s = \gamma \cdot P_{heat} \cdot t \quad (3)$$

In order to analyze the maximum thermal damage characteristics of the cable, the finite element software ANSYS

molecular chain to break, accelerating the aging of the cable insulation layer material, on the other hand, there is a certain difference in the temperature on both sides of the cable, frequent and large temperature changes are more likely to cause cable insulation material fatigue. Taking the high temperature side of the aircraft cable as the research object, the surrounding thermal environment is equivalent to a one-sided heat source with uniform heating and negligible thickness at a distance of d from the cable. The cable is simplified to a concentric cylinder with conductor radius r_1 and total radius r_2 . The principle of the cable thermal influence and the cable structure are shown in Fig.2.

is used to simulate the temperature distribution of the insulation layer of the cable. Through the temperature distribution, we can find that the isothermal surface temperature of the insulation part of the cable is equal to the melting point and diffused in an approximate hemispherical manner, and the maximum damage depth is radial. Literature [30] analyzes the damage characteristics of cables under the influence of arc heat release, and also verifies the conclusion of hemispherical damage shape. The heat source in [30] is one-sided as the same as ours, but the instantaneous temperature is higher, and the duration is shorter.

The finite element analysis software ANSYS is used to simulate the temperature distribution of the insulation part under the influence of a constant one-sided heat source, and the isothermal surface of the cable insulation part temperature is equal to the melting point diffuses in an approximate hemispherical way, as shown in Fig.3. The initial condition is that the temperature of the insulated part of the cable is equal to the ambient temperature without applying a heat source, without considering the thermal radiation between the faces.

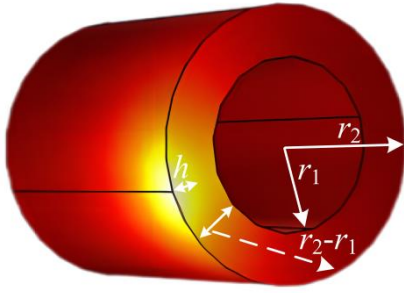


Fig.3. Temperature distribution of cable insulation layer under heat transfer

Assuming that all the heat absorbed by the cable is converted into the melting volume of the insulator, further calculate the melting volume V and melting depth h of the insulation layer:

$$V = \frac{E_s}{(T_m - T_a) \cdot c \cdot \rho} = \frac{\gamma \cdot P_{heat} \cdot t}{(T_m - T_a) \cdot c \cdot \rho} \quad (4)$$

$$h = \sqrt[3]{\frac{3E_s}{2\pi \cdot (T_m - T_a) \cdot c \cdot \rho}} = \sqrt[3]{\frac{3\gamma P_{heat} t}{2\pi(T_m - T_a)c\rho}} \quad (5)$$

Where the melting depth is equal to the radius of the isothermal surface formed by the melting point at this time, where T_m and T_a respectively represent the melting temperature and the ambient temperature, ρ , c and t respectively represent the density, heat capacity of the insulation layer and heat source influence time.

2.3. Definition of cable thermal damage features

Based on the mechanism of cable thermal damage, two types of cable thermal damage characteristics is defined from the influence and degree to support efficient and accurate safety analysis.

(1) Thermal Damage Influence Factor

According to the analysis in Section 2.1, the relationship between cable damage depth and the 1/3 power of heat absorption is approximately linear. Considering the influence of heat absorption, heat dissipation and working time on cable thermal damage, the cable thermal damage influence factor α_{pd} is defined.

$$\alpha_{pd} = \left(1 - \frac{K_T K_{TS} \tau}{5\tau_0}\right)^{1/3} \quad (6)$$

In the formula, τ_0 is the rated cable life, τ is the working time, K_{TS} is the thermal influence factor, K_T is the temperature acceleration failure factor, and 5 is the ultimate service life multiplier.

The cable thermal influence factor K_{TS} is defined from the perspective of temperature cycle change during flight, the

improved Norris-Landzberg model [31] is used to define and reflect the destructiveness of temperature cycle with a long period.

$$K_{TS} = \left(\frac{24}{N_0} \times \frac{Ns}{t_a}\right) \times \left(\frac{\min(\theta_s, 2)}{\min(\theta_0, 2)}\right)^{\frac{1}{3}} \times \left(\frac{\Delta T_s}{\Delta T_0}\right)^{0.6} \times e^{1414 \times \left(\frac{1}{273+T_0+\Delta T_0} - \frac{1}{T_{s-max}+273}\right)} \quad (7)$$

where Ns is the number of annual cycles, N_0 is the number of reference cycles, t_a is the total duration of a specific phase in a year, θ_c is the actual cycle duration (in hours), θ_0 is the reference cycle duration, ΔT_s and ΔT_0 represent the actual and reference amplitudes of the temperature cycle, T_0 and T_{s-max} represent the reference temperature and the maximum temperature during the temperature cycle, and 0.6 is fatigue coefficient of the material used for the cable insulation.

The temperature acceleration failure factor K_T is defined from the angle of maximum heat absorption, which can reflect the maximum solar radiation intensity.

$$K_T = \mu P_R T_R t_R \quad (8)$$

Where P_R , T_R and t_R are summer solar radiation amount, summer average temperature and summer average sunshine time. The proportional coefficient μ is used as an index to evaluate the applicability of the life prediction method. The smaller the difference of the proportional coefficients calculated from different regions, the more stable the life prediction method is, and the greater the adaptability and extensibility of the method.

(2) Radial Melting Rate

In order to more intuitively evaluate the influence of thermal damage depth on cable safety and characterize the melting degree of aircraft cable, the ratio of melting depth h to the thickness of the insulating part of aircraft cable ($r_2 - r_1$) is defined as the radial melting rate η :

$$\eta = \begin{cases} \frac{h}{r_1 - r_2} \times 100\% = \\ \frac{1}{r_2 - r_1} \sqrt[3]{\frac{3\gamma P_{heat} \tau}{2\pi(T_m - T_a)c\rho}} \times 100\%, h < (r_2 - r_1) \\ 1, h \geq (r_2 - r_1) \end{cases} \quad (9)$$

When calculating the melting depth h , only the propagation of temperature in the insulation part is considered, while not considering the limit of the thickness of the insulation part. It may be the case that h is numerically greater than the thickness of the insulation part ($r_2 - r_1$). When h is numerically greater than ($r_2 - r_1$), heat will be transferred to the surrounding insulation

materials. Therefore, the maximum radial melting rate η is 1, which means the temperature of the insulation reaches the melting point at the radial length (r_2-r_1) .

3. Cable life prediction based on thermal damage influence factor

Thermal damage destroys the spatial structure of the insulation layer of the cable, reduces the insulation performance of the cable, and increases the failure probability of the cable. When thermal damage is not considered, after obtaining the rated failure rate λ_1 , the mean time between failure calculation (MTBF) is calculated [32].

$$MTBF_0 = \int e^{-\lambda_1 \tau} d\tau \quad (10)$$

Thermal damage influence factor is used to indicate that cable thermal damage accelerates cable failure, and combined with the thermal damage influence factor and rated failure rate, an improved calculation method of cable MTBF is proposed.

$$MTBF_1 = \int e^{-\lambda_1 \tau} \alpha_{pd} d\tau \quad (11)$$

FIDES is a kind of actual failure rate correction model of electronic devices considering the influence of manufacturing, environment and other factors, which is widely used in the life prediction of mechanical and electronic products [33-34]. In order to further validate the effectiveness of the cable life prediction method based on thermal damage influence factors, the FIDES model life prediction method and the life prediction method of FIDES combined with thermal damage factors will be used as a control group. Considering the temperature, humidity, vibration and other factors in operation, the corrected aircraft cable failure rate λ_2 is calculated using the FIDES model. The detailed process of the correction method is shown in Appendix A, and the environmental data of the aircraft at different stages are shown in Table A in the Appendix, and $MTBF_2$ is calculated as follows.

$$MTBF_2 = \int e^{-\lambda_2 \tau} d\tau \quad (12)$$

Without considering the effect of operating temperature, the corrected aircraft cable failure rate λ_3 is calculated by using FIDES model. The detailed process of the correction method is shown in Appendix B, and $MTBF_3$ combined with thermal damage influence factor is calculated as follows.

$$MTBF_3 = \int e^{-\lambda_3 \tau} \alpha_{pd} d\tau \quad (13)$$

Literature [26] lists the actual MTBF and actual failure rates

of a certain type of aircraft cable in eight cities from 2012 to 2014, as shown in Table 1. The rated values of MTBF and failure rate of this type of aircraft cable are 175,200h and 5.71×10^{-6} respectively.

Table 1. Failure data of a certain type of aircraft cable from 2012-2014

Operating Area	Actual MTBF($\times 10^4$ h)	Actual $\lambda(\times 10^{-6})$
Guangdong	13.14	7.61
Hainan	13.14	7.61
Shanxi	11.356	8.81
Heilongjiang	9.567	10.5
Xinjiang	9.56	10.5
America	13.143	7.61
Europe	14.379	6.95
Africa	14.379	6.95

Aircraft operation can be divided into three main stages: take-off, cruise and landing. In the cruise stage, the altitude of the aircraft is 6000~8000 meters, and the environmental parameters are the same, so different regions of the aircraft cable operating environment is mainly reflected in the take-off and landing stage. Since meteorological data such as airport areas are difficult to obtain, we use geographic data from public data sets to approximately replace aircraft operation environmental data. The daily temperature, humidity and other meteorological data of the representative cities in the eight cable operating areas from 2012 to 2014 are obtained from the National Oceanic and Atmospheric Administration's National Center for Environmental Information[35], and data of similar years are used to replace the missing data in some areas, as shown in Appendix C.

When combining the thermal damage influence factor to predict the cable life, the aircraft cable failure data in Guangdong region is first used to solve the proportional coefficient μ , and then the cable life in the remaining seven operating regions is predicted. Comparison of the life predicted results and errors of different life prediction methods are shown in Fig.4, and the proportionality coefficient μ is obtained from the cable environment and life data solving in different operating regions, as shown in Table 2, and comparison of the values of μ in the different method is shown in Table 3.

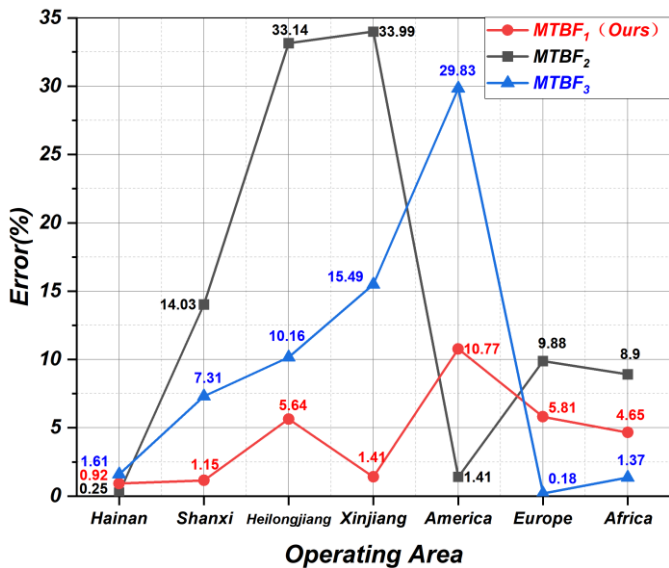


Fig.4. Cable life errors solved by different methods

The results show that our proposed lifetime prediction

Table 2. The values of μ solved by different methods ($\times 10^{-4}$)

	Guangdong	Hainan	Shanxi	Heilongjiang	Xinjiang	America	Europe	Africa
$MTBF_1$	2.1353	2.1863	2.1802	2.3474	2.1879	2.9366	1.7619	1.8315
$MTBF_3$	3.5232	3.6730	3.2703	3.4037	2.9537	6.8716	2.9071	3.0769

Table 3. Comparison of the values of μ ($\times 10^{-4}$)

	Range	Average	Standard Deviation
$MTBF_1$	1.1747	2.1959	0.3579
$MTBF_3$	3.9645	3.7099	1.3058

The results show that our proposed lifetime prediction method ($MTBF_1$) has a low error, especially for aircraft cables operating in a single city in China, and the error is significantly lower than the other two methods. For America, Europe and Africa, where the operating area is larger and the climate conditions are more complex, we propose that the error fluctuation of the life prediction method is small, and the error is less than 10%, which is at an acceptable level.

At the same time, the calculation results of the proportional coefficients of different cities also show that the μ value of our proposed life prediction method is stable at 2×10^{-4} , however, the μ value in the method of $MTBF_3$ fluctuates greatly, which also proves that our proposed method has stronger applicability and can be further extended to the study of cable life prediction in other operating areas.

Comparison of the three methods proves that the cable life prediction method combined with the thermal damage influence

method ($MTBF_1$) has a low error, especially for aircraft cables operating in a single city in China, and the error is significantly lower than the other two methods. For America, Europe and Africa, where the operating area is larger and the climate conditions are more complex, we propose that the error fluctuation of the life prediction method is small, and the error is less than 10%, which is at an acceptable level.

At the same time, the calculation results of the proportional coefficients of different cities also show that the μ value of our proposed life prediction method is stable at 2×10^{-4} , however, the μ value in the method of $MTBF_3$ fluctuates greatly, which also proves that our proposed method has stronger applicability and can be further extended to the study of cable life prediction in other operating areas.

factor is more accurate, and has stronger applicability to the life prediction of different operating regions. The life prediction method can guide the operation of the cable to ensure the maintenance, replacement and failure prevention.

4. Cable risk dynamic assessment based on dual indexes

4.1. Dual index nonlinear risk classification

During the operation of aircraft cables, there may be operating or environmental conditions beyond the scope of the design specifications, and the cable risk level may be higher than the set standards. Conducting a risk assessment to determine the cable risk status can provide input for developing reasonable risk responses and help decision makers develop improvement measures to ensure that the system is always within an acceptable risk range. It is worth noting that failure risk is a comprehensive evaluation of failure probability, severity of failure and other factors, and failure risk assessment solely based on failure probability may result in results contrary to facts [36].

The failure risk of thermal damage to the cable insulation layer is reflected in two aspects. On the one hand, high temperature accelerates the aging of the insulation layer and

increases the probability of cable insulation failure. On the other hand, the radial melting of the cable insulation layer destroys the physical structure of the cable and increases the severity of the cable failure. Aiming at the continuous operation process of cable, a risk dynamic assessment model for aircraft cable with radial melting rate η and failure probability F as indicators is constructed. The calculation method of failure probability F_0 without considering the influence of thermal damage and failure probability F_1 considering the influence of thermal damage are calculated as follows.

$$F_0 = 1 - e^{-\lambda_0\tau} \quad (14)$$

$$F_1 = 1 - e^{-\lambda_0\tau}\alpha_{pd} \quad (15)$$

Risk level classification is the basis for risk dynamic assessment. With a single index, AC25.1309-1B [37] and Guo Jiayin [38] proposed a risk classification method based on failure probability and cable aging state, respectively. The two single indicator risk assessment level intervals are shown in Table 4.

Table 4. Risk level interval divided by different indexes

Index	Risk Level				
	Safe	Low	Middle	High	Very High
η	[0,0.3]	(0.3,0.5]	(0.5,0.7]	(0.7,1]	/
F	[0,0.2]	(0.2,0.4]	(0.4,0.6]	(0.6,0.8]	(0.8,1]

When evaluating on the basis of failure probability and

radial melting rate at the same time, the linear risk assessment method represented by the risk priority number multiplies the two types of factors directly to obtain the risk level [39]. However, there may be an unreasonable situation in which the same risk assessment result is obtained from the "high failure probability and light failure result" and the "low failure probability and serious failure result". Therefore, referring to the nonlinear risk assessment method in SAE J1739 [40], a four-interval nonlinear risk level model construction method for cable thermal damage risk assessment is proposed. While retaining the original evaluation results of low risk and medium risk level, the original high risk is divided into two intervals with equal ranges: high risk and very high risk. The D-S evidence theory method is used to fuse the two types of risk indicators including failure probability and melting rate, and obtain the risk values [41]. The solution method is as follows.

$$F = 1 - R \quad (16)$$

$$\Theta = \eta(1 - F) + F(1 - \eta) \quad (17)$$

$$RI = \frac{\eta F}{1 - \Theta} \quad (18)$$

Where RI is the fused risk value. Referring to the risk division method of the highest two types of risk interval which approximately satisfies 2:3 in [38], the original high risk is further refined according to the RI value ranking result. The risk levels divided by the different methods are shown in Fig.5.

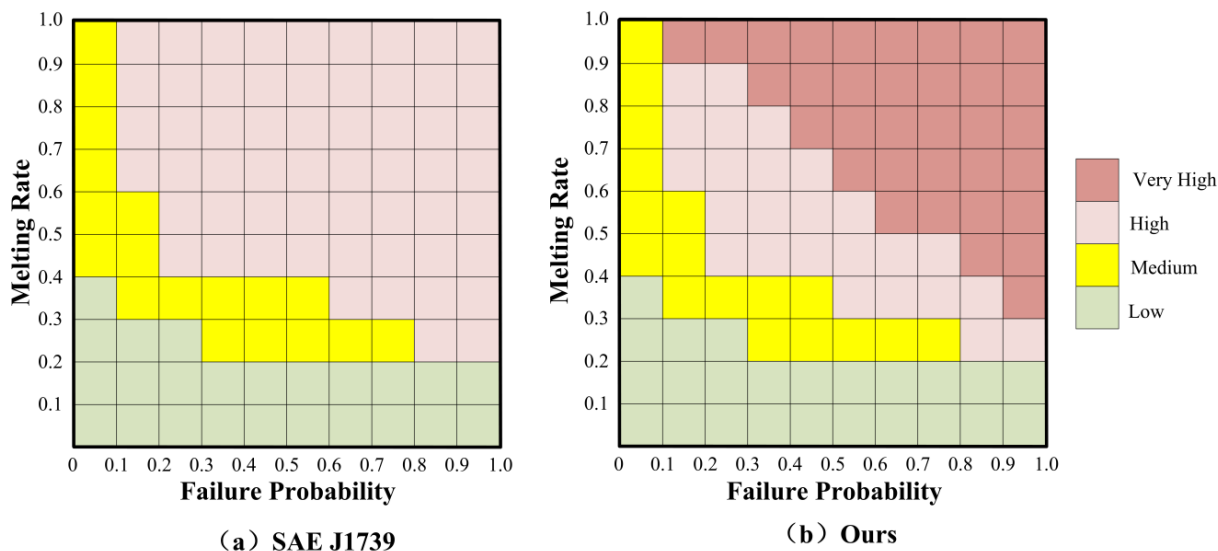


Fig.5. Four-interval nonlinear risk level graph divided by two indexes.

4.2. Case analysis of aircraft cable risk assessment

In section 4.5.2 of literature [42], pp. 81-84, the failure characteristics of a kind of XPLE cable under thermal radiation

are analyzed. By analyzing the experimental data, it is found that under the same thermal radiation intensity, the insulation failure time of the cable will shorten with the increase of service life. When influenced by the heat radiation intensity of

5.4kW/m², the aircraft cable will fail in a short time. The cable has been working normally for 25.8 years, the normal working temperature is 60 °C, the insulation failure temperature is 232 °C, the thickness of the cable sheath layer and the insulation layer are 0.2218cm and 0.1615cm respectively, and the outer diameter is 1.0380cm. The material is 0.92g/cm³, the specific heat capacity is 2.2J/(g·K), and the cable is rated for 40 years. It is estimated that the ambient heat transfer coefficient γ remains unchanged and is equal to 1, and the radial melting rate corresponding to the absorbing power P_{heat} of the insulated part of the cable surface and 3.5s is:

$$P_{heat} = 5400 \times 10^{-6} \times \pi \times 10.38^2 = 1.83W \quad (19)$$

$$\eta = \frac{1}{0.2218 + 0.1615} \sqrt[3]{\frac{3 \times 1 \times 1.83 \times 3.5}{2\pi(232 - 60) \times 2.2 \times 0.92}} \times 100\% = 52.81\% \quad (20)$$

The equivalent thermal damage factor of the test cable after normal operation and high temperature test is approximately replaced by the cable thermal damage factor in the strongest thermal radiation intensity in Section 3, and the cable failure probability F_0, F_1 are calculated:

$$F_0 = 1 - e^{-\lambda_0 t} = 1 - e^{-\frac{25.8}{40}} = 0.4753 \quad (21)$$

$$F_1 = 1 - e^{-\lambda_0 \tau} \left(1 - \frac{K_T K_{TS} \tau}{5\tau_0}\right)^{1/3} = 1 - e^{-\frac{25.8}{40}} \left(1 - \frac{1.7958 \times 2.4123 \times 25.8}{5 \times 40}\right)^{1/3} = 0.6006 \quad (22)$$

The cable risk assessment results obtained by different indicators are shown in Table 5. Based on the radial melting rate η and failure probability F_0 , the cable is considered to be *Medium Risk*. Based on the failure probability considering the thermal damage F_1 and the radial melting rate with failure probability $\eta+F_0$, the cable is considered to be *High Risk*. However, considering the failure probability calculated by thermal damage and radial melting rate $\eta+F_1$, the cable is considered to be *Very High Risk*, which is consistent with the experimental phenomenon of "immediate failure in a short time", proving the effectiveness of the proposed dual-index risk assessment method. The risk assessment results of the two different combination analyses are shown in Fig.6.

Table 5. Risk assessment results

Index	η	F_0	F_1	$\eta+F_0$	$\eta+F_1$
Risk Level	Medium	Medium	High	High	Very High

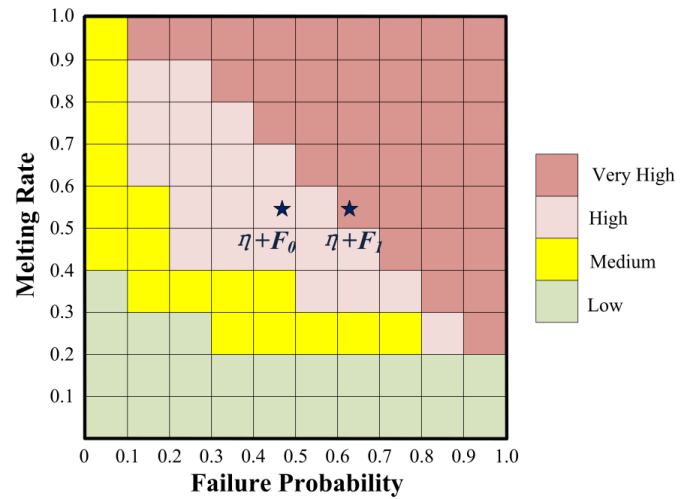


Fig.6. Cable risk level assessment results

5. Conclusion

This paper starts with the analysis of the thermal failure mechanism of aircraft cable, then defines two types of cable safety characteristics including thermal damage impact factor and radial melting rate, and puts forward the construction method of cable life prediction model and cable risk assessment method. The main conclusions are as follows.

i)The definition of cable thermal damage characteristics and its safety analysis method based on failure mechanism are reasonable and effective.

ii)The proposed cable life prediction method based on thermal damage influence factor requires less data, and owes higher accuracy and better applicability.

iii)The dual-index nonlinear evaluation model of radial melting rate and failure probability is reasonable and effective, and the evaluation results are in agreement with the experimental results.

iv)The proposed feature-based safety method can provide a reference for the safety analysis of other systems. The proposed life prediction provides a new idea for other systems and components, and the dual index nonlinear risk assessment model also provides a reference for the dynamic security assessment of the system.

The method proposed needs to be validated on more cable failure data in the future, and risk assessment studies on different cable types need to be carried out. We will also try to extend the proposed life prediction and risk assessment methods to the performance of airborne equipment such as transformer rectifiers.

Acknowledgments

The authors would like to thank the referees for their valuable comments and useful suggestions that help them to greatly improve the paper, and the support from the China Scholarship Council, National Natural Science Foundation of China and the Civil Aviation Joint Research Fund of the Civil Aviation Administration of China under the project number U2233205 & U2133203 and the Postgraduate Research & Practice Innovation Program of Jiangsu Province under the project number KYCX23_0390.

References

1. Chen Y, Hui B, Cheng Y, et al. Effects of connection conditions between insulation screen and Al sheath on the buffer layer failures of high-voltage XLPE cables. *Engineering failure analysis*. 2021;122:105263, <https://doi.org/10.1016/j.engfailanal.2021.105263>.
2. Liu J, Yan S, Wang S, et al. Evaluation of Electrical Tree Aging State of XLPE Cables Based on Low Frequency and High Voltage Frequency Domain Spectroscopy. *Transactions of China Electrotechnical Society*. 2023;38(9): 2510-2518, <https://doi.org/10.19595/j.cnki.1000-6753.tces.212081>.
3. Andruszkiewicz J, Lorenc J, Łowczowski K, Weychan A, Zawodniak J. Energy losses' reduction in metallic screens of mv cable power lines and busbar bridges composed of single-core cables. *Eksploatacja i Niezawodność-Maintenance And Reliability*. 2020;22:15-25, <https://doi.org/10.17531/ein.2020.1.3>.
4. Yang Haoqi. Research on Intelligent Assessment Method of Aviation DC Arc Risk. Master's dissertation in Nanjing University of Aeronautics and Astronautics. 2023.
5. Zhang Yuemei. Research on Health Status Assessment and Remaining Life Prediction for Spacecraft Power System. Master's dissertation in Nanjing University of Aeronautics and Astronautics, <https://doi.org/10.27239/d.cnki.gnhhu.2021.000468>.
6. Zhang S, Zhang Y. Nonlinear mixed reliability model with non-constant shape parameter of aviation cables. *Applied mathematical modelling*. 2021;96:445-455, <https://doi.org/10.1016/j.apm.2021.03.011>.
7. Zhao G, Di H, Bai H, Lin Y. A cable health assessment method based on multi-agent and matter-element extension model. *Sustainable energy technologies and assessments*. 2023;56:103108, <https://doi.org/10.1016/j.seta.2023.103108>.
8. Okpokparoro S, Sriramula S. Reliability analysis of floating wind turbine dynamic cables under realistic environmental loads. *Ocean engineering*. 2023;278:114594, <https://doi.org/10.1016/j.oceaneng.2023.114594>.
9. Bukya M, Kumar R, Gupta RK. A study on safety issues and analytical evaluation of stresses for HVDC cable in electrical vehicle. *AIP Conference Proceedings*. 2020;2294, <https://doi.org/10.1063/5.0031351>.
10. Diban B, Mazzanti G. The effect of temperature and stress coefficients of electrical conductivity on the life of HVDC extruded cable insulation subjected to type test conditions. *IEEE transactions on dielectrics and electrical insulation*. 2020;27:1313-1321, <https://doi.org/10.1109/TDEI.2020.008772>.
11. Yang Ping. Study on improved electrical life model of DC cable insulation materials based on performance attenuation. Master's dissertation in Chongqing University of Technology, <https://doi.org/10.27753/d.cnki.gcqgx.2021.000737>.
12. Liao Y, Bao S, Xie Y, et al. Breakdown failure analysis of 220 kV cable joint with large expanding rate under closing overvoltage. *Engineering failure analysis*. 2021;120:105086, <https://doi.org/10.1016/j.engfailanal.2020.105086>.
13. Zhu H, Han Z, Yang J, et al. Multi-factor simulation analysis of operation characteristics of side-by-side directly buried cables. *Electric power systems research*. 2023;218:109143, <https://doi.org/10.1016/j.epsr.2023.109143>.
14. Long M, Fang H, Yuege Z, et al. Research on Life Assessment Method of Spacecraft Optical Cable Based on Degradation Data. 2019 Prognostics and System Health Management Conference (PHM-Qingdao). IEEE; 2019:1-6, <https://doi.org/10.1109/PHM-Qingdao46334.2019.8942891>.
15. Yu X, Ai T, Wang K. Application of nanogenerators in acoustics based on artificial intelligence and machine learning. *APL Materials*. MELVILLE: AIP Publishing; 2024;12:2-16, <https://doi.org/10.1063/5.0195399>.
16. Zhan X, Liu Z, Yan H, et al. A novel method of health indicator construction and remaining useful life prediction based on deep learning. *Eksploatacja i Niezawodność*. 2023;25(4):171374, <https://doi.org/10.17531/ein/171374>.
17. Santhosh TV, Gopika V, Ghosh AK, Fernandes BG. An approach for reliability prediction of instrumentation & control cables by artificial neural networks and Weibull theory for probabilistic safety assessment of NPPs. *Reliability engineering & system safety*. 2018;170:31-

- 44,<https://doi.org/10.1016/j.ress.2017.10.010>.
18. Pan Q, Zhang C, Wei X, et al. Assessment of MV XLPE cable aging state based on PSO-XGBoost algorithm. *Electric power systems research*. 2023;221:109427,<https://doi.org/10.1016/j.epsr.2023.109427>.
 19. Hu Y, Huang C, Zhang D, et al. Cable Life Prediction Based on BP Neural Network. 2021 International Conference on Networking Systems of AI (INSAI). *IEEE*; 2021:258-262,<https://doi.org/10.1109/INSAI54028.2021.00055>.
 20. Li D, Wang X, Wu J, et al. XLPE cable insulation aging based on feature detection life prediction method. *Journal of Electric Power Science and Technology*. 2022;37(01):168-177,<https://doi.org/10.19781/j.issn.1673-9140.2022.01.020>.
 21. Gao J, Yang D, Wang S, et al. State of health estimation of lithium-ion batteries based on Mixers-bidirectional temporal convolutional neural network. *Journal of energy storage*. 2023;73:109248,<https://doi.org/10.1016/j.est.2023.109248>.
 22. Liu Y, Li Q, Wang K. Revealing the degradation patterns of lithium-ion batteries from impedance spectroscopy using variational auto-encoders. *Energy Storage Materials*. 2024;69,<https://doi.org/10.1016/j.ensm.2024.103394>.
 23. Fang P, Sui X, Zhang A, et al. Fusion model based RUL prediction method of lithium-ion battery under working conditions. *Eksploatacja i Niezawodność – Maintenance and Reliability*. 2024;<https://doi.org/10.17531/ein/186537>.
 24. Jin H, Hu Y, Ge H, et al. Remaining useful life prediction for lithium-ion batteries based on an improved GWO-SVR algorithm. *Chinese Journal of Engineering*. 2024;46(03):514-524,<https://doi.org/10.13374/j.issn2095-9389.2023.05.31.002>.
 25. Hou Q, Cao L, Shan T, et al. Remaining useful life prediction of aviation lithium battery based on indirect health index and echo state network. *Measurement & Control Technology*. 2022;41(07):57-63,<https://doi.org/10.19708/j.ckjs.2021.12.304>.
 26. Qiu Senbao. Research on reliability management of a company's aviation cable. Master's dissertation in South China University of Technology. 2016.
 27. International Electrotechnical Commission. IEC60227-1: Polyvinyl chloride insulated cables of rated voltages up to and including 450/750V-Part 1:General requirements. 2007.
 28. State Administration for Market Regulation (China), Standardization Administration (China). GB/T 42096: Performance requirements for aircraft fire-resisting electrical cables. 2022.
 29. European Committee for Standardization. EN 3475-100: Aerospace series - Cables, electrical, aircraft use - Test methods - Part 100: General. 2010.
 30. Meng Z, Wang L, Sun J, et al. Parallel arc damage modeling in aircraft system. *Transactions of China Electrotechnical Society*. 2015;30(22):263-268,<https://doi.org/10.19595/j.cnki.1000-6753.tces.2015.22.032>.
 31. FIDES guide 2009 Edition A. Reliability methodology for electronic systems. <http://www.fides-reliability.org>.
 32. Selech J, Rogula-Kozłowska W, Piątek P, et al. Failure and reliability analysis of heavy firefighting and rescue vehicles: a case study. *Eksploatacja i Niezawodność – Maintenance and Reliability*. 2024;26(1),<http://doi.org/10.17531/ein/175505>.
 33. Chen C, Li B, Guo J, Liu Z, Qi B, Hua C. Bearing life prediction method based on the improved FIDES reliability model. *Reliability engineering & system safety*. 2022;227:108746,<https://doi.org/10.1016/j.ress.2022.108746>.
 34. Miad A, Aditya S, Pavol B. Comparison of Military Handbook and the FIDES Methodology for Failure Rate Estimation of Modular Multilevel Converters. 2023 IEEE 17th International Conference on Compatibility, Power Electronics and Power Engineering (CPE-POWERENG). 2023:1-6, <https://doi.org/10.1109/CPE-POWERENG58103.2023.10227449>.
 35. Index of /data/global-summary-of-the-day/archive.<https://www.ncei.noaa.gov/data/global-summary-of-the-day/archive/>.
 36. Xiong Minlan. Research on Operational Risk of Civil Aircraft Based on Data and Cases. Master's dissertation in Nanjing University of Aeronautics and Astronautics. 2021.
 37. Federal Aviation Administration. AC 25.1309-1B System Design and Analysis. 2002.
 38. Guo Jiayin. Research on Fire Risk Assessment and Online Monitoring System of Power Cable. Master's dissertation in China University of Mining and Technology. 2022,<https://doi.org/10.27623/d.cnki.gzkyu.2022.001149>.
 39. Society of Automotive Engineers. SAE ARP4761A: Guidelines and methods for conducting the safety assessment process on civil airborne systems and equipment. 2023.
 40. Society of Automotive Engineers. SAE J1739: Potential Failure Mode and Effects Analysis (FMEA) Including Design FMEA, Supplemental FMEA-MSR, and Process FMEA. 2021.

41. Xu J, Ding R, Li M, et al. A new Bayesian network model for risk assessment based on cloud model, interval type-2 fuzzy sets and improved D-S evidence theory. *Information sciences*. 2022;618:336-355, <http://doi.org/10.1016/j.ins.2022.11.011>.
42. Li Jinmei. Research on the cable failure characteristics and prediction method under fire conditions. Doctoral dissertation in University of Science and Technology Beijing. 2018.
43. Gao Cheng, Chen Bingyin, Huang Jiaoying, et al(2020). Research on Failure Rate Prediction of MEMS Based on FIDES with Multiple Failure Mechanisms. *JOURNALS: Microelectronics*, vol.20, no.05, pp.743-749, <https://doi.org/10.13911/j.cnki.1004-3365.190631>.

Appendix A: Calculation methods of MTBF2

The FIDES model proposed by eight French companies, including Airbus, Eurocopter and Thales Aeronautical Systems, belongs to a failure physical model, which respectively calculates the accelerated aging factors of electronic devices under the action of environmental factors such as temperature, temperature cycle, relative humidity and mechanical vibration [31]. On this basis, the failure rate based on the actual working environment is obtained by modifying the basic failure rate. Considering the effects of four environmental factors, the four types of environmental accelerated aging factors are defined in the FIDES model.

i) Define the temperature accelerated aging factor π_T based on the Arrhenius equation.

$$\pi_T = e^{\frac{E_a}{K_B}(\frac{1}{T_1} - \frac{1}{T_2})} \quad (\text{A-1})$$

where E_a is the activation energy, Boltzmann's constant K_B equals 8.617×10^{-5} eV/K, and T_1 and T_2 represent the reference temperature and ambient temperature.

ii) Define the temperature damage factor π_{T-s} based on the modified Norris-Landzberg model to simulate temperature cycles, which can reflect the destructiveness of temperature cycles with longer periods.

$$\pi_{T-s} = \left(\frac{24}{N_0} \times \frac{N_s}{t_a}\right) \times \left(\frac{\min(\theta_s, 2)}{\min(\theta_0, 2)}\right)^{\frac{1}{3}} \times \left(\frac{\Delta T_s}{\Delta T_0}\right)^{0.6} \times e^{1414 \times \left(\frac{1}{273+T_0+\Delta T_0} - \frac{1}{T_{s-max}+273}\right)} \quad (\text{A-2})$$

where N_s is the number of annual cycles, N_0 is the number of reference cycles, t_a is the total duration of a specific phase in a year, θ_c is the actual cycle duration (in hours), θ_0 is the reference cycle duration, ΔT_s and ΔT_0 represent the actual and reference amplitudes of the temperature cycle, T_0 and T_{s-max} represent the reference temperature and the maximum temperature during the temperature cycle, and 0.6 is fatigue coefficient of the material used for the cable insulation.

iii) Define the relative humidity insulation failure factor π_H based on the Peck model to simulate the accelerated failure of cables under the combined effect of relative humidity and temperature.

$$\pi_H = \left(\frac{H_a}{H_0}\right)^p \times e^{11604 \times E_a \times \left(\frac{1}{273+T_1} - \frac{1}{T_2+273}\right)} \quad (\text{A-3})$$

where H_a is the ambient relative humidity, H_0 is the reference humidity, and p is the humidity stress acceleration factor.

iv) Define the vibration acceleration aging factor π_V based on the actual amplitude and reference amplitude.

$$\pi_H = \left(\frac{H_a}{H_0}\right)^p \times e^{11604 \times E_a \times \left(\frac{1}{273+T_1} - \frac{1}{T_2+273}\right)} \quad (\text{A-4})$$

Where G_V and G_{V0} represent the actual amplitude and reference amplitude respectively, and 1.5 is the mechanical stress aging acceleration factor.

The aircraft cable failure rate correction model can be expressed as follows:

$$\lambda = \lambda_0 \cdot \pi_{PM} \cdot \pi_{process_2} \quad (\text{A-5})$$

Where λ_0 is the theoretical failure rate, λ is the actual failure rate, π_{PM} is the manufacture coefficient, which is generally obtained by the inverse solution of the failure rate or the quality grade estimation, and $\pi_{process_2}$ is the environment failure coefficient. Defined Π_j as the environmental coefficient weight vector, then the expression of the environment failure coefficient is as follows.

$$\pi_{process_2} = \Pi_a \cdot \Pi_j = (\pi_T, \pi_{T-s}, \pi_H, \pi_V) \cdot (j_T, j_{T-s}, j_H, j_V)^T \quad (\text{A-6})$$

The value of the weight vector (j_T, j_{T-s}, j_H, j_V) is $(0.7, 0.1, 0.1, 0.1)^T$, which refers to literature [43]. After the failure rate is obtained,

the reliability and mean time between failure (MTBF) of the aircraft cable are further calculated.

$$MTBF_2 = \int_0^{+\infty} e^{-\lambda_2 t} dt \quad (A-7)$$

When solving for the physical factors accelerated aging factor, the analysis is performed in five phases: ground parking, ground stopping, ground taxiing, takeoff/approach, and smooth flight. In the ground parking stage, all kinds of airborne systems do not work, and only the influence of ambient temperature and humidity are considered. In the ground stopping stage, passengers are mainly boarded and alighted, and all kinds of airborne systems work, while the aircraft does not displace, and the influence of mechanical vibration factors is not considered. In the ground taxiing stage, the aircraft slides at low speed and there is no violent bump, so that the value of mechanical vibration is smaller. The information of each stage is shown in Table A.

Table A. Information on different stages of the aircraft over a year

	Stage				
	Ground Parking	Ground Stopping	Ground Taxiing	Takeoff/ Approach	Smooth Flight
Duration(Hour/Year)	3230	700	630	1050	3150
Temperature(°C)	Same as environment	40	40	40	40
RH(%)	environment	30	10	10	10
$\Delta T(^{\circ}C)$	$0.5(T_D - T_N)$	—	—	—	—
Cycles(/Year)	365	730	1460	1460	1460
Duration(Hour/Cycle)	8.9	0.96	0.43	0.72	2.16
Vibration(Grms)	—	—	0.6	5	0.6

Appendix B: Calculation methods of MTBF₃

The calculation method of environmental accelerated aging factor is the same as that in Appendix A. Considering factors such as humidity and vibration during operation, the aircraft cable failure rate failure rate correction model can be expressed as:

$$\lambda_3 = \lambda_0 \cdot \pi_{PM} \cdot \pi_{process_3} \quad (B-1)$$

$$\pi_{process_3} = \Pi_a \cdot \Pi_j = (\pi_H, \pi_V) \cdot (j_H, j_V)^T \quad (B-2)$$

The value of the weight vector (j_H, j_V) is $(0.5, 0.5)^T$, which also refers to literature [44]. After obtaining the failure rate, further calculate the reliability and MTBF of the cable:

$$MTBF_3 = \int e^{-\lambda_3 t} dt \quad (B-3)$$

Appendix C: Operating regional representative city meteorological data

Table C. Operating regional representative city meteorological data

Representative City	GuangZhou	Sanya	Taiyuan	Harbin	Kashi	New York	London	Cairo	
DT (°C)	SP	26.84	28.06	20.58	14.31	20.77	9	10	27.51
	SU	32.75	29.71	29.17	27.76	31.4	24	20	33.95
	AU	27.99	27.18	16.97	12.51	19.54	23	19	26.77
	WI	17.56	23.29	1.68	-8.88	0	7	9	18.36
NT (°C)	SP	19.75	21.83	7.02	0.30	9.41	1	4	13.18
	SU	24.89	24.17	18.32	17.04	18.66	16	11	20.65
	AU	19.50	21.52	4.50	1.60	5.95	15	11	15.68
	WI	10.58	17	-8.58	-23.1	-9.03	0	4	7.46
RH (%)	SP	75	80	42	50	35	65	75	50
	SU	80	85	50	70	30	70	70	55
	AU	75	80	45	65	35	65	75	50
	WI	65	75	38	60	35	60	80	50
SRI (MJ/m ²)	19	21	17	16	21	15	14	16	
LDS (h)	13	13.5	15	17	16	14.5	15	13	

Where DT is daytime temperature, NT is night temperature, RH is relative humidity, SP, SU, AU, WI are short for spring, summer, autumn and winter, SRI is summer radiation intensity, LDS is length of daylight in summer.